

MYBBP1A-mediated IGFBP4 promoter methylation promotes epithelial-mesenchymal transition and metastasis through activation of NOTCH pathway in liver cancer

YUJING SUN^{1*}, XIAOYU WENG^{2*}, WEI CHEN³, JIANGZHEN GE², BO DING², JUNNAN RU², YUNGUO LEI⁴, XIN HU⁴, DA MAN², SHAOBING CHENG⁵, RUOSHU DUAN¹, JINGJING REN¹ and BENG YANG²

¹Department of General Practice, The First Affiliated Hospital, School of Medicine, Zhejiang University, Hangzhou, Zhejiang 310003, P.R. China; ²Division of Hepatobiliary and Pancreatic Surgery, Department of Surgery, The First Affiliated Hospital, School of Medicine, Zhejiang University, Hangzhou, Zhejiang 310003, P.R. China; ³General Practice Department, The Second Affiliated Hospital of Zhejiang Chinese Medical University, Hangzhou, Zhejiang 310005, P.R. China; ⁴Zhejiang University School of Medicine, Hangzhou, Zhejiang 310058, P.R. China; ⁵Department of Colorectal Surgery, The First Affiliated Hospital, School of Medicine, Zhejiang University, Hangzhou, Zhejiang 310003, P.R. China

Received January 26, 2024; Accepted November 8, 2024

DOI: 10.3892/ijo.2024.5710

Abstract. Metastatic hepatocellular carcinoma (HCC) seriously threatens patients' prognosis. It was previously suggested that the insulin growth factor binding protein (IGFBP) family could serve as cancer suppressors in the development and metastasis of HCC. However, the role of IGFBP4 and its underlying molecular mechanism in HCC metastasis is elusive. In the present study, it was found that IGFBP4 is significantly downregulated in HCC, whose expression is positively correlated with the prognosis of patients with HCC. Overexpression of IGFBP4 restrained

migration abilities and cancer metastasis of HCC cells both *in vitro* and *in vivo*. Furthermore, it was found that IGFBP4 represses HCC metastasis by inhibiting epithelial-mesenchymal transition. Molecular mechanism studies showed that overexpression of IGFBP4 obviously suppresses NOTCH1 signaling in HCC. As for the upstream regulatory mechanism, it was revealed that downregulation of IGFBP4 in HCC was caused by CpG islands' hyper-methylation-dependent degradation mediated by MYBBP1A. Inhibition of MYBBP1A limited HCC metastatic ability and silence of IGFBP4 at the same time restored HCC metastatic potentials. Clinical data demonstrated that low expression of IGFBP4 was found in patients with HCC, especially with lymphatic metastasis. High MYBBP1A expression and low IGFBP4 expression in HCC were correlated with poor survival of patients with HCC. Summarily, in the present study, it was revealed that MYBBP1A/IGFBP4/NOTCH1 pathway could play a crucial role in the progression and metastasis of HCC, which stimulates novel therapeutic and diagnostic strategies against metastatic HCC.

Correspondence to: Dr Beng Yang, Division of Hepatobiliary and Pancreatic Surgery, Department of Surgery, The First Affiliated Hospital, School of Medicine, Zhejiang University, 79 Qingchun Road, Shangcheng, Hangzhou, Zhejiang 310003, P.R. China
E-mail: 21518093@zju.edu.cn

Professor Jingjing Ren, Department of General Practice, The First Affiliated Hospital, School of Medicine, Zhejiang University, 79 Qingchun Road, Shangcheng, Hangzhou, Zhejiang 310003, P.R. China
E-mail: 3204092@zju.edu.cn

*Contributed equally

Abbreviations: HCC, hepatocellular carcinoma; IGFBP, insulin-like growth factor binding protein; IGF, insulin-like growth factor; MYBBP1A, Myb-binding protein 1A; EMT, epithelial-mesenchymal transition; TCGA, The Cancer Genome Atlas; GTEx, The Genotype-Tissue Expression; GSEA, Gene Set Enrichment Analysis; RT-qPCR: reverse transcription-quantitative polymerase chain reaction; WB, western blotting; IHC, immunohistochemistry; OE, overexpression; WT, wild-type; BSP, bisulfite sequencing PCR; OS, overall survival; DSS, disease-specific survival

Key words: HCC, IGFBP4, metastasis, EMT, MYBBP1A

Introduction

Hepatocellular carcinoma (HCC) is the fifth most common malignant tumor worldwide and the second leading cause of cancer-related deaths globally (1,2). HCC accounts for 85-90% of all primary liver cancers (3). In 2022, there were over 430,000 newly reported cases of liver cancer in China, ranking fourth among all cancers, with over 410,000 deaths, ranking second among all cancer-related deaths (4). Despite significant advances in liver resection, liver transplantation, radiotherapy, chemotherapy and immunotherapy in recent years, the prognosis for patients with HCC remains poor due to high recurrence and metastasis rates, as well as resistance to chemotherapy and targeted therapy (5,6). Therefore, it is urgent to clarify the mechanisms of HCC metastasis and identify new therapeutic targets.

Insulin-like growth factor binding proteins (IGFBPs) are a group of secreted proteins that can bind to insulin-like

growth factors (IGFs). They mainly include IGFBP1-7, which can affect the binding strength between IGF and IGF receptor (IGFR) and subsequently regulate the activation of downstream signaling pathways, thus controlling the growth and proliferation of target cells (7). According to the significant differences in expression levels of all IGFBPs between tumors and normal tissues, combining survival analysis, IGFBP4 has drawn our attention. Previous studies have showed that IGFBP4 is involved in the development of multiple diseases such as lung cancer (8), breast cancer (9), bladder epithelial cancer (10), bone metabolism (11) and endocrine metabolic diseases (12). However, its role and specific mechanisms in HCC have not been clearly defined.

In the present study, it was identified that IGFBP4 is downregulated in liver cancer. The expression of IGFBP4 was associated with a favorable prognosis in patients with liver cancer. Functionally, IGFBP4 inhibited cell migration and invasion *in vitro* and suppressed tumor metastasis *in vivo*. Mechanistically, the expression of IGFBP4 is regulated by MYBBP1A, which targeted the methylation of the IGFBP4 promoter region to suppress its transcription, thereby affecting its expression. IGFBP4 could inhibit NOTCH pathway activation, furthermore inhibit epithelial-mesenchymal transition (EMT) and impact tumor metastasis. Additionally, MYBBP1A and IGFBP4 expression could be combined to predict poor prognosis in HCC. In summary, the present study expands the knowledge of the regulation of IGFBP4 mediated by MYBBP1A, reveals a new mechanism in HCC tumorigenesis and demonstrates its potential for precise diagnosis.

Materials and methods

Patients and specimens. The present study adhered to the ethical guidelines outlined in the Declaration of Helsinki (1964), and protocols were approved (approval no. 2020-IIT-834) by the Ethics Committee of The First Affiliated Hospital of Zhejiang University (Hangzhou, China). All patients included in the study provided written informed consent. Surgical specimens of liver cancer tissue samples and adjacent non-tumor tissue samples of 25 patients with HCC with or without metastasis were retrospectively collected from The First Affiliated Hospital of Zhejiang University, between January 2015 and December 2019. The patients were randomly selected based on specific clinical and pathological criteria, including confirmed diagnosis of HCC, stages I-III according to the Barcelona Clinic Liver Cancer (BCLC) classification, and no previous treatment. The age of the patients (22 men and 3 women) ranged from 37-80 years, with a median age of 60 years. Demographic data were recorded but did not influence selection criteria. The clinicopathological characteristics of the 25 patients are listed in Table S1. Following surgical resection, tissue samples were immediately snap-frozen in liquid nitrogen and stored at -80°C to preserve RNA integrity. All samples were processed using standardized protocols for RNA extraction to ensure high-quality analysis.

Bioinformatics analysis. The transcript expression data and survival information of the Liver HCC (LIHC) from The Cancer Genome Atlas (TCGA) and the gene expression data in Genotype-Tissue Expression (GTEx; <https://gtexportal.org/home/>) were used for the present study. The Kaplan-Meier plotter website (<https://kmplot.com/analysis/>), the GEPIA website (<http://gepia.cancer-pku.cn>), and the UALCAN website (<https://ualcan.path.uab.edu/>) were used to analyze the clinical correlations with MYBBP1A and IGFBP4. The Methprimer database (<http://www.urogene.org/methprimer/>) was used to predict the methylation sites of IGFBP4 and it was found that there were CpG islands in the promoter region of IGFBP4. The SMART website (<http://www.bioinfo-zs.com/smartapp/>) was used to analyze the correlations of expression and methylation of IGFBP4. Genes were ranked based on their correlation with IGFBP4 expression levels. Differentially expressed genes (DEGs) were identified using standard thresholds of $P < 0.05$ and $|\log_2 \text{FC}| > 1$. These DEGs were then subjected to differential expression analysis and gene set enrichment analysis (GSEA) to explore the potential pathways and biological processes associated with IGFBP4.

Cell lines and cell culture. The human liver cancer cell lines HCCLM3 (cat. no. TCHu270), Huh7 (cat. no. TCHu182) as well as HepG2 (cat. no. TCHu72) used in the present study were obtained from the Cell Bank of the Chinese Academy of Sciences Typical Culture Collection Committee. Prior to use, all cell lines were validated by short tandem repeat (STR). Cells were maintained and stored according to the provider's instructions. The culture medium contained 10% fetal bovine serum (FBS; BioInd; <http://www.bioind.org/>), 100 IU/ml penicillin and 100 IU/ml streptomycin. Cells were cultured in a humidified incubator at 37°C with 5% CO₂.

Reagents and drugs treatment. Referring to previous studies (13), different concentrations (0, 5, 10 and 40 $\mu\text{mol/l}$) of the methylation inhibitor Decitabine (5-Aza-2'-deoxycytidine) (cat. no. HY-A0004; MedChemExpress) dissolved in DMSO were used to inhibit the methylation process. After 48 h of treatment, the cells were collected for western blotting (WB) and reverse transcription-quantitative PCR (RT-qPCR).

Lentivirus construction and cell transfection. MYBBP1A-RNAi-lentivirus, IGFBP4-RNAi-lentivirus and IGFBP4-overexpression (oe) lentivirus were purchased from Shanghai GeneChem Co., Ltd. pFU-GW-016-hU6-MCS-CBh-gcGFP-IRES-puromycin was used as the vector for shMYBBP1A and shMYBBP1A control. MYBBP1A shRNA sequences were targeted: 5'-GCTGGTGAATGTGCTGAA GATGGCC-3'; pFU-GW-014-hU6-MCS-Ubc-mCherry-IRES-neomycin was used as the vector for shIGFBP4 and shIGFBP4 control. IGFBP4 shRNA sequences were targeted: 5'-CTG CAGAAGCACTTCGCCAAA-3'; in addition, a random sequence control shRNA, 5'-TTCTCCGAACGTGTCACG T-3' was used as a negative control (NC). pGC-FU-CMVenhancer-3FLAG-EF1-ZsGreen1-T2A-puromycin was used as the vector for oeIGFBP4 and its control was vector only control.

All lentivirus constructs were generated using second-generation lentiviral vector packaging system provided by Shanghai GeneChem Co., Ltd. Packaging was performed using the helper plasmids Helper1.0 and Helper2.0 (Shanghai GeneChem Co., Ltd.). 293T cells (cat. no. GNHu17; Cell Bank of the Chinese Academy of Sciences Typical

Culture Collection Committee) were transfected with the lentiviral constructs (target vector plasmid 20 μg , Helper1.0 vector plasmid 15 μg , Helper2.0 vector plasmid 10 μg) using Lipofectamine 2000 (Thermo Fisher Scientific, Inc.) according to the manufacturer's protocol. Cells were incubated at 37°C with 5% CO₂ for 48 h post-transfection. After 48 h, the viral supernatant was collected, filtered through a 0.22- μm filter, and concentrated by ultracentrifugation at 73,000 x g for 2 h at 4°C.

The viral particles were harvested and used to transduce the target cells Huh7 and HCCLM3. The target cells were infected at a multiplicity of infection of 10, and Polybrene (Shanghai GeneChem Co., Ltd.) was added at a final concentration of 4 $\mu\text{g}/\text{ml}$ to improve the infection efficiency. After incubation at 37°C for 8–12 h, the complete medium was replaced. A total of 48 h after infection, cells were selected using puromycin or neomycin (3–4 $\mu\text{g}/\text{ml}$) (Sangon Biotech Co., Ltd.) for 72 h and transfection efficiency was confirmed by RT-qPCR and WB.

RNA extraction and RT-qPCR. Cell and tissue total RNA were extracted using an RNA-Quick Purification Kit (Esunbio; <http://www.esunbio.com/>). Total RNA was reverse transcribed into cDNA with HiScript II Q Select RT SuperMix for qPCR (cat. no. R233-01; Vazyme Biotech Co., Ltd.) and HiScript III All-in-one RT SuperMix Perfect for qPCR (cat. no. R333-01; Vazyme Biotech Co., Ltd.) according to the manufacturer's protocol. RT-qPCR was performed with ChamQ SYBR Green Master Mix (Vazyme Biotech Co., Ltd.) on QuantStudio 5 Real-Time PCR System (Thermo Fisher Scientific, Inc.). After pre-denaturation at -95°C for 5 min, the reaction was carried out at 95°C for 10 sec and at 60°C for 30 sec, with 40 cycles. The expression of target genes was calculated using the $2^{-\Delta\Delta C_q}$ method and normalized to the expression of GAPDH (14). The primers of all genes were ordered from TsingKe Biological Technology and listed in Table SII.

WB assays. Whole cells or tissues were lysed with RIPA buffer (Wuhan Servicebio Technology Co., Ltd.) supplemented with protease and phosphorylation inhibitor cocktail (Selleck Chemicals) and quantified by BCA Protein Assay Kit (Thermo Fisher Scientific, Inc.). Then a total of 30 μg of protein loaded per lane were electrophoresed with 4–20% SDS-PAGE (GenScript) and transferred to 0.22- μm PVDF membranes (MilliporeSigma). Membranes were blocked with 5% BSA (Beijing Solarbio Science & Technology Co., Ltd.) or 25% non-fat milk for 1 h at room temperature, and incubated with primary antibodies over 8 h or overnight in 4°C. After being washed with TBST (with 0.1% Tween) and incubated for 1 h with secondary antibodies at room temperature, the protein bands were exposed to an ECL detection reagent (Fudebio; <http://www.fudebio.com/>) in the chemiluminescence system (Bio-Rad Laboratories, Inc.). GAPDH was marked as an internal control. Quantification of WB bands was performed using ImageJ software (version 1.54k; National Institutes of Health). The 'Analyze Gel' tool in ImageJ was used to measure the grayscale intensity of protein bands. Signal intensity for each band was background-corrected and normalized to the internal control protein for relative quantification. All information regarding antibodies used in WB is included in Table SIII.

Immunohistochemistry (IHC). The metastatic tumors and liver tissues from mice and clinical patients were fixed with 4% paraformaldehyde at room temperature for 48 h and embedded in paraffin. The tissue sections were cut to a thickness of 3 μm and followed by H&E and IHC staining (incubation with the E-cadherin, N-cadherin and Vimentin antibodies at 4°C for 8 h) respectively. The tissue sections were stained with H&E (Wuhan Servicebio Technology Co., Ltd.) at room temperature for 5 and 7 min, respectively. The IHC assay was performed as previously described (15). Product information and dilution ratios of primary antibodies is provided in Table SIII.

Immunofluorescence (IF). Cells (10x10⁴ cells/well) were seeded onto glass coverslips in a 6-well plate and allowed to adhere overnight at 37°C with 5% CO₂. The cells were washed twice with PBS and fixed with 4% paraformaldehyde at room temperature for 20 min. After two washes with PBS, the cells were stained with 5 $\mu\text{g}/\text{ml}$ iFluor™ 488 phalloidin (cat. no. 40736ES75; Shanghai Yeasen Biotechnology Co., Ltd.) at room temperature for 60 min, followed by two PBS washes. The cells were incubated with 1 $\mu\text{g}/\text{ml}$ DAPI (cat. no. 40728ES50; Shanghai Yeasen Biotechnology Co., Ltd.) at room temperature for 10 min. After two additional PBS washes, fluorescence images were captured under a fluorescence microscope.

Transwell assays. Cells (5x10⁴ cells/well) suspended in serum-free medium were seeded into each upper Transwell chamber (24 well 8.0- μm pore size; Falcon; Corning Life Sciences), while medium containing 10% FBS was added to the lower chamber. After incubation for 72 h at 37°C with 5% CO₂, the migratory or invasive cells in the lower chambers were fixed at room temperature for 10 min with 4% paraformaldehyde and stained at room temperature for 15 min with 0.1% crystal violet. Migratory cells were plotted as the average number of cells per field of view using a light microscope (Olympus Corporation) from 3 independent experiments.

Gap closure assays. Cells (5x10⁴ cells/well) were seeded into both sides of Culture-Inserts® (Ibidi GmbH) to make a 500- μm gap. After incubation for 48 h in Huh7 and 72 h in HCCLM3 cells, inserts were removed to allow cell migration for the indicated period of time in serum-free medium. Migration distances were plotted as the average distance of two sides of cells views using a light microscope (Olympus Corporation) from 3 independent experiments.

Colony formation assay. Cells (1x10³ cells/well) were seeded into 6 well plates and incubated for 2–3 weeks at 37°C with 5% CO₂. Then, the colonies on the plates were fixed at room temperature for 10 min with 4% polyoxymethylene and stained at room temperature for 15 min with 0.1% crystal violet. Viable colonies (>50 cells) were observed and counted manually and are pictured. The numbers of colonies are depicted as bar graphs. All experiments were repeated three times under the same conditions and methods.

DNA methylation analysis by bisulfite sequencing. The genomic DNA of cells was extracted using the standard phenol-chloroform technique followed by proteinase K treatment to prevent protein contamination. Bisulfite conversion was performed using an EpiTect Fast DNA Bisulfite

Kit (cat. no. 59824; Qiagen China Co., Ltd.) according to the manufacturer's protocol. The bisulfite-treated genomic DNA was subjected to PCR for the amplification of the CpG islands of IGFBP4 promoter using Hot Start Takara Taq DNA Polymerase (Takara Biotechnology Co., Ltd.). Amplified PCR products were cloned into the pGEMT-easy vector using DNA Ligation Kit (cat. no. 6022; Takara Biotechnology Co., Ltd.). A total of 10 insert-positive clones were isolated by the QIAprep Spin Miniprep kit (cat. no. 27104; Qiagen China Co., Ltd.). RNA sequencing and analysis of the samples were performed by Hangzhou Cosmos Wisdom Biotech Co. The PCR primers used for bisulfite sequencing of CpG islands of the promoter region of IGFBP4 gene are presented as follows: forward, 5'-TTYGGTAGAAAAGGATTTTATAGATG-3' and reverse, 5'-CACRAAACAAAAACAACATAACC-3'.

Tumor xenograft model. A splenic venous liver metastasis tumor experiment was performed with male immunodeficient nude mice aged 5 weeks and weighing 20–25 g. A total of 5 mice in each group were purchased from the Zhejiang Academy of Medical Sciences and raised in the SPF barrier of the Experimental Animal Center of the First Affiliated Hospital of Zhejiang University School of Medicine with 12/12-h light-dark cycle, 21–23°C and a relative humidity of 60–65%, with *ad libitum* access to food and water, with *ad libitum* supply of food and water. Experiments were performed in strict accordance with the NIH Guide for the Care and Use of Laboratory Animals. A total of 10 BALB/c nude mice were randomly allocated into two groups. After careful sterilization, 75 μ l PBS containing 5x10⁶ Huh7 cells of IGFBP4 stabilized-knockdown or control cells were injected in the spleen of mice. The detailed process was conducted as previously described (16). Experimental nude mice were anesthetized by intraperitoneal injection of pentobarbital sodium according to their body weight (50 mg/kg). After anesthesia, tumor cells were injected under the splenic capsule for compression, hemostasis and suture. After injection, the mental state, abdominal shape and weight of the mice were observed every week to evaluate the tumor progression. In our laboratory animal Centre, experienced animal care staff monitored the animals daily and notified the laboratory staff if anything unusual happened. If the mice showed obvious wasting, lethargy and significant abdominal distension or where the ascites burden exceeded 10% of the body weight (17), the humane experimental endpoint was reached. Their whole liver was removed when the mice were euthanized and immediately processed for histological evaluation. For a total of 60 days after injection, all mice were administered peritoneal injections of pentobarbital (150 mg/kg) and euthanized by cervical dislocation. Cardiac arrest is then followed by a pulsar examination to confirm death. The liver metastasis model was constructed for previous research proposes (18–23). The animal studies were approved (approval no. 2020-IIT-rapid-1132) by the Clinical Research Ethics Committee of the First Affiliated Hospital, School of Medicine, Zhejiang University (Hangzhou, China).

Statistical analysis. All experiments were repeated three times under the same conditions and methods to ensure the repeatability of the experiment. All data are expressed as

the mean \pm standard deviation (SD). Significant differences between the two unpaired groups were tested by the unpaired Student's t-test, and paired groups were tested using paired t-test. The one-way ANOVA test followed by Tukey's post hoc test was used to analyze comparisons of significant differences between three or more groups. Kaplan-Meier and log-rank tests were performed to determine survival. The correlation analysis was evaluated using Pearson's test. In all statistical analyses, *P<0.05 was considered to indicate a statistically significant difference. Statistical analysis of data was performed using GraphPad Prism 8.0.2 software (Dotmatics).

Results

Expression of IGFBP4 is reduced in HCC tissues and negatively correlated with poor prognosis in patients with HCC. To determine which IGFBP family member may be the key to regulating HCC progression, the IGFBPs family (IGFBP1–7) gene expression was first analyzed using TCGA-LIHC datasets. The results showed that the IGFBP1 (P<0.001), IGFBP3 (P<0.001), IGFBP4 (P<0.001) and IGFBP5 (P=0.0042) have significantly downregulated expression in liver cancer (Fig. 1A). Kaplan-Meier plotter website was used to predict the single gene expression associated with HCC prognosis, and low expression of IGFBP4 (P=2.1x10⁻⁶) and IGFBP7 (P=2.2x10⁻⁵) was found; rather, other IGFBP members were significantly correlated with poor prognosis of patients with LIHC (Fig. 1B). Thus, further studies were performed to investigate the role of IGFBP4 in HCC progression. The expression of IGFBP4 was found to be lower in the HCC population compared with the normal population, especially in the Asian population (Fig. 1C). In addition, the expression of IGFBP4 was further reduced in patients with HCC with poor liver tumor grade and lymph node metastasis (Fig. 1D and E). The downregulated expression of IGFBP4 in the clinical tumor specimens of patients with HCC was further validated using RT-qPCR (P<0.0001) and WB (Fig. 1F and G). IHC staining also demonstrated that IGFBP4 expression was lower in HCC tissues compared with that in the matched adjacent normal tissues (Fig. 1H). These data indicated that IGFBP4 was downregulated in HCC and its low expression predicts poor prognosis in patients with HCC.

IGFBP4 inhibits the metastatic ability of liver cancer cells through repressing EMT. To explore the biological function of IGFBP4 in liver cancer, its expression levels were first assessed in various liver cancer cell lines. The results showed high IGFBP4 expression in HCCLM3 cells, moderate expression in MHCC97H and HepG2 cells, and low expression in Huh7 cells (Fig. 2A and B). HCCLM3 and Huh7 were selected for further study. IGFBP4 overexpression lentivirus was applied in Huh7 and HCCLM3 cells, and the transfection efficiency was proven at both the mRNA and protein levels (Fig. 2C and D). The Transwell assays revealed that IGFBP4 overexpression inhibited the migration ability in both two cell lines *in vitro* (Fig. 2E). Moreover, gap closure assays also showed that IGFBP4-overexpressing Huh7 and HCCLM3 cell lines decreased migration ability (Fig. 2F). In addition, overexpression of IGFBP4 could also

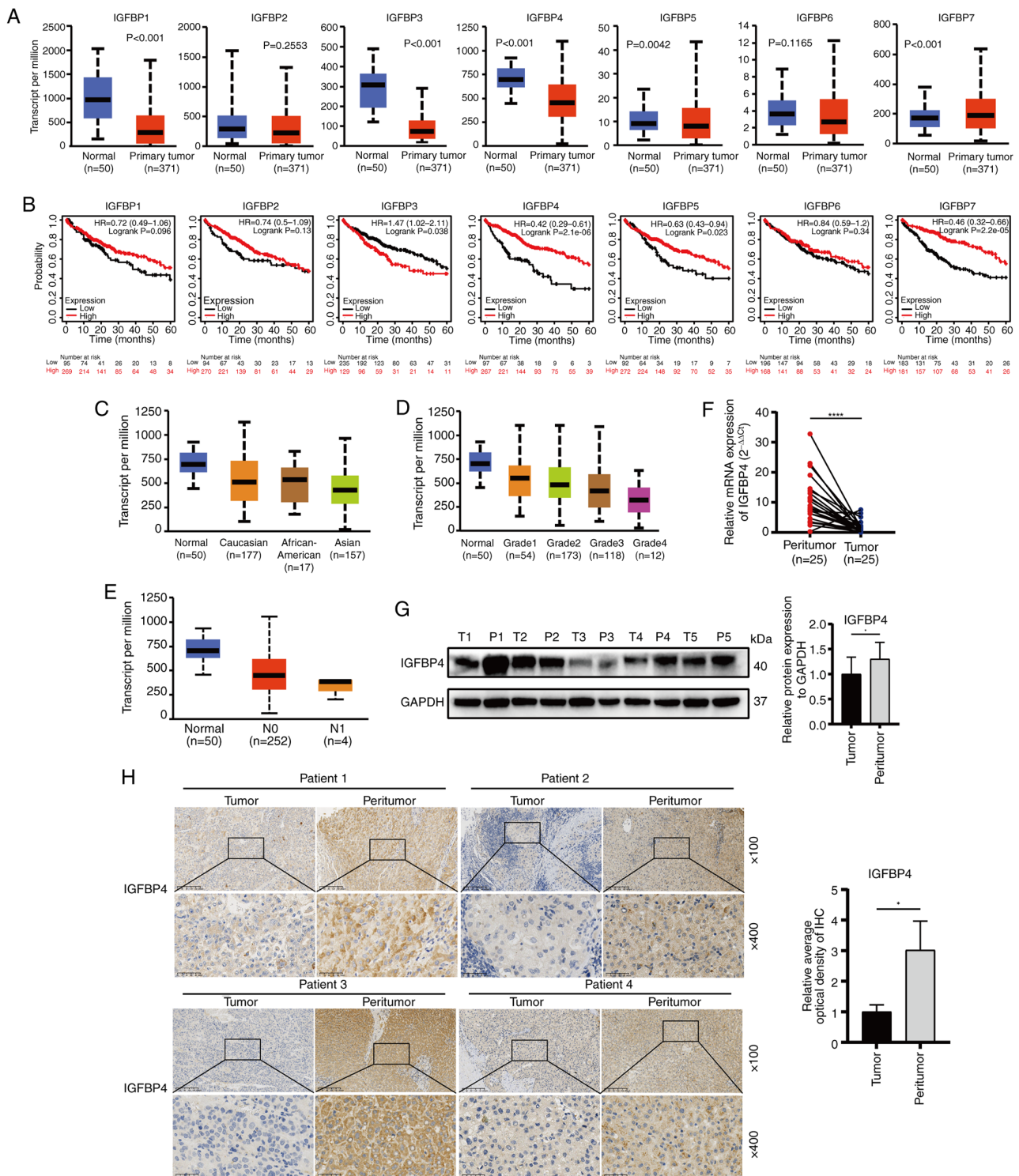


Figure 1. Expression of IGFBP4 is downregulated in HCC. (A) Expression of IGFBP1 to IGFBP7 in normal and primary tumor patients based on LIHC in the TCGA and Genotype-Tissue Expression databases. (B) Kaplan-Meier survival analyzed patient survival in different expression groups of IGFBP1 to IGFBP7 in TCGA-LIHC [log-rank (Mantel-Cox)]. (C) Expression of IGFBP4 in patients from various ethnicities based on LIHC in the TCGA databases. (D and E) Expression of IGFBP4 based on different tumor grades and nodal metastasis of LIHC in TCGA databases. (F) IGFBP4 mRNA expression in paired HCC tissues (n=25) and adjacent non-tumor tissues (n=25) evaluated by reverse transcription-quantitative PCR (****P<0.0001, paired t-test). (G) Representative IGFBP4 protein expression results in paired HCC tissues and adjacent non-tumor tissues evaluated by western blotting (*P<0.05, paired t-test). (H) Representative immunohistochemical images of IGFBP4 staining in liver tumor or adjacent tissues (scale bar, 100 μm; magnification, x100, and x400; *P<0.05, paired t-test). IGFBP, insulin-like growth factor binding protein; HCC, hepatocellular carcinoma; LIHC, liver hepatocellular carcinoma; TCGA, The Cancer Genome Atlas.

reduce proliferation ability of liver cancer cells (Fig. S1). Phalloidin staining results showed that NC liver cancer cells appeared more rounded and had fewer pseudopodia compared with those with IGFBP4 overexpression (Fig. 2G).

Cancer metastasis is closely related to the EMT of tumor cells. WB was used to verify EMT-associated protein expression. IGFBP4 ectopic overexpression increased the expression of E-cadherin while decreasing the expression

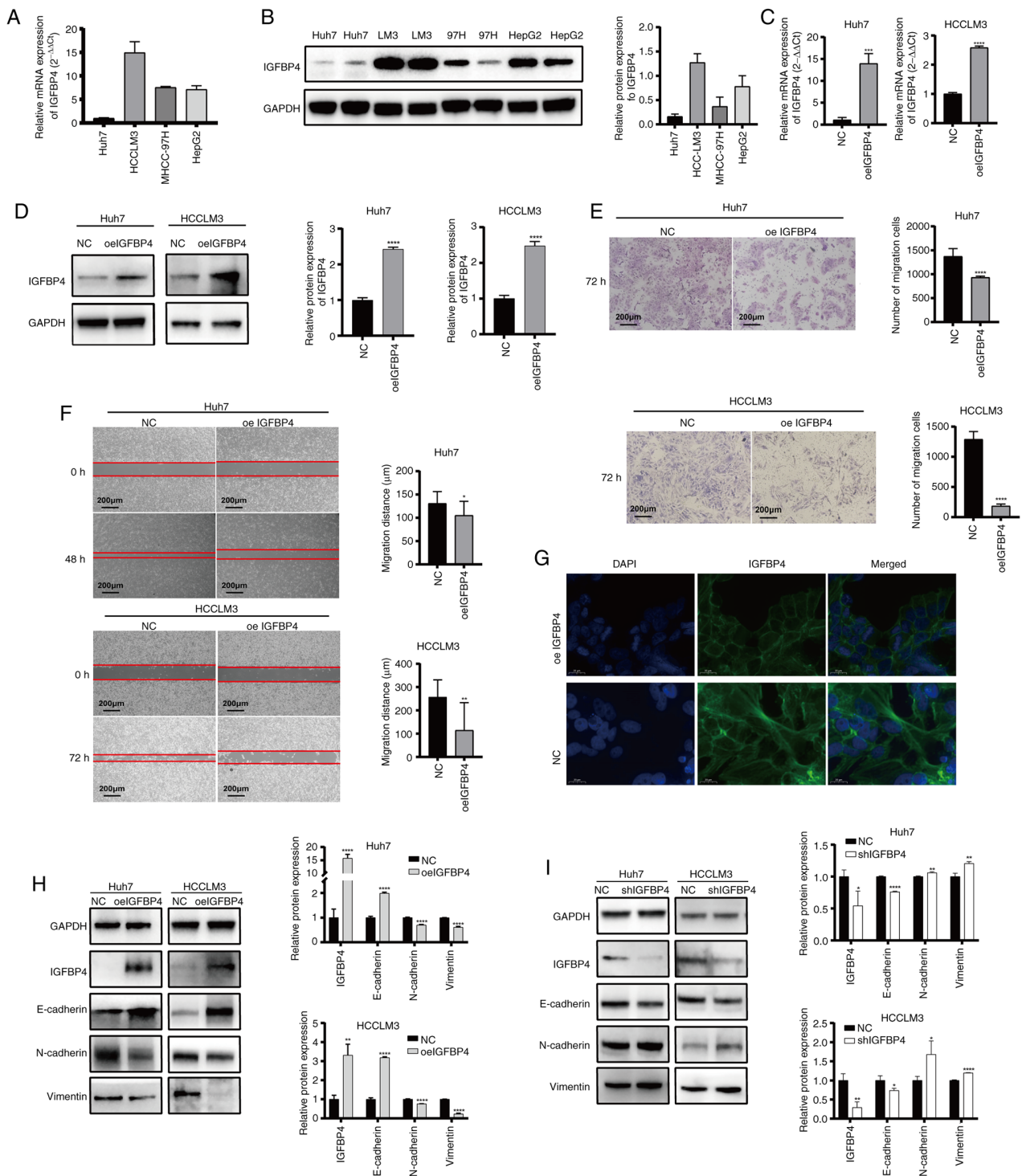


Figure 2. IGFBP4 inhibits the metastatic ability of liver cancer cells through repressing epithelial-mesenchymal transformation *in vitro*. (A and B) Basal expression of IGFBP4 in mRNA level and protein level in Huh7, HCCLM3, MHCC-97H and HepG2 cell lines by RT-qPCR and WB. (C) The mRNA levels of IGFBP4 in Huh7 and HCCLM3 cell lines after transfection with IGFBP4-oe lentivirus based on RT-qPCR (** $P < 0.001$ and **** $P < 0.0001$, Student's t-test). (D) The protein expression of IGFBP4 in Huh7 and HCCLM3 cell lines after transfection with IGFBP4-oe lentivirus based on WB (**** $P < 0.0001$, Student's t-test). (E and F) The migratory abilities of oeIGFBP4 Huh7 and HCCLM3 cells based on (E) Transwell migration assays and (F) gap closure assays, respectively (original magnification, $\times 100$ and $\times 400$; * $P < 0.05$, ** $P < 0.01$ and **** $P < 0.0001$, Student's t-test). (G) The cytoskeletal morphologic effects of overexpressing IGFBP4 in liver cancer cells were detected by phalloidin staining (phalloidin, green; DAPI, blue; scale bar, 50 μm). (H) The protein levels of E-cadherin, N-cadherin, Vimentin and IGFBP4 in NC and oeIGFBP4 Huh7 and HCCLM3 cells based on WB (** $P < 0.01$, **** $P < 0.0001$, Student's t-test). (I) The protein levels of E-cadherin, N-cadherin, Vimentin and IGFBP4 in shIGFBP4 and NC groups in Huh7 and HCCLM3 cells based on WB (* $P < 0.05$, ** $P < 0.01$, **** $P < 0.0001$, Student's t-test). IGFBP4, insulin-like growth factor binding protein 4; RT-qPCR, reverse transcription quantitative PCR; WB, western blotting; oe-, overexpression; sh-, short hairpin; NC, negative control.

of N-cadherin and Vimentin in HCCLM3 and Huh7 cells (Fig. 2H). By contrast, IGFBP4 silencing increased the expression of N-cadherin and Vimentin, whereas it

decreased the expression of E-cadherin (Fig. 2I). All these results suggested that IGFBP4 can alter the cytoskeleton and repress EMT in liver cancer cells.

The silencing of IGFBP4 increased tumor metastasis in vivo. To further investigate whether IGFBP4 promotes tumor metastasis *in vivo*, a splenic venous liver metastasis model was constructed by injecting lentivirus-mediated shRNA targeting IGFBP4 transduced cells and control cells under the splenic envelope of nude mice to mimic the liver metastasis (Fig. 3A). More liver metastatic nodules were found in IGFBP4-knockdown group (Fig. 3B). Interestingly, intestinal metastasis was accidentally found in one IGFBP4 knockdown mice (Fig. S2). H&E staining showed the microstructure of metastatic lesions (Fig. 3C). Moreover, among normal liver tissues, it was also found that low expression of IGFBP4 in the liver was accompanied by low E-cadherin expression and high N-cadherin expression, and vice versa (Fig. 3D). These results demonstrated that IGFBP4 silencing promotes cancer cell metastasis *in vivo*.

IGFBP4 inhibits the activation of the NOTCH signaling pathway. To explore the mechanism of IGFBP4 in regulating liver cancer malignancy, differentially expressed genes (DEGs) enrichment analysis (Fig. 4A) and GSEA analysis were performed, and the NOTCH pathway was found enriched (Fig. 4B). NOTCH signaling is a strong modulator in regulating the EMT process (24-26), thus it was hypothesized that IGFBP4 might inhibit EMT through the NOTCH pathway. RT-qPCR was used to verify the mRNA expression level of core genes of the NOTCH pathway, which are involved in the present GSEA analysis. It was found that mRNA levels of NOTCH receptor 1 (NOTCH1), hes family bHLH transcription factor 1 (HES1) and neuralized E3 ubiquitin protein ligase 1 (NEURL) decreased after IGFBP4 overexpression, and increased after IGFBP4 silencing (Fig. 4C and D). WB results showed that overexpression of IGFBP4 reduced the expression of NOTCH1 and HES1 at the protein level, while knockdown of IGFBP4 had the opposite effect (Fig. 4E and F). Next, to verify the relation of NOTCH pathway activation and IGFBP4 expression in the liver, IHC was performed. IHC results revealed that NOTCH1 expression was reduced in the liver tissue with high levels of IGFBP4, and vice versa (Fig. 4G). The Smad and β -catenin pathways play crucial roles in EMT and tumor metastasis, which is well established. WB assays were performed to assess the expression levels of β -catenin, Wnt3a, Smad2/3 and phosphorylated Smad2/3. However, no significant alterations were observed in the expression of these proteins following IGFBP4 overexpression (Fig. S3). Additionally, the expression changes of the transcription factor YAP1 in the NOTCH signaling pathway were assessed. It was found that the protein expression level of YAP1 was significantly reduced in liver cancer cells with IGFBP4 overexpression, and the level of YAP1 was positively correlated with the activation of the NOTCH pathway (Fig. S4). These results showed that IGFBP4 overexpression could inhibit the NOTCH signaling pathway activation in liver cancer cells.

IGFBP4 is negatively regulated by MYBBP1A via CpG island methylation-mediated degradation. Our previous study had shown that IGFBP5, another important IGFBP family member, could be regulated by MYBBP1A and inhibit the metastasis ability of liver cancer cells (13). Thus, it was hypothesized that IGFBP4 may be regulated by MYBBP1A as

well. In order to investigate the relation between MYBBP1A and IGFBP4, though analyzing the data from the TCGA database and GTEx database, it was found that the IGFBP4 gene expression varied obviously when the expression of MYBBP1A was changed (Fig. 5A). At the same time, a correlation analysis between two genes was conducted and it was identified that there was no significant correlation between the expression of MYBBP1A and IGFBP4 in the liver tissue of the normal liver tissue ($P=0.5$, $R=0.098$) (Fig. 5B). However, a negative correlation of MYBBP1A and IGFBP4 expression was observed in liver tumor tissues of patients with HCC ($P=9.8 \times 10^{-6}$, $R=-0.23$) (Fig. 5C). The experimental results demonstrated that MYBBP1A knockdown resulted in a significant increase in the mRNA and protein expression level of IGFBP4 (Fig. 5D and E). By contrast, after overexpressing MYBBP1A, IGFBP4 decreased in both mRNA and protein levels (Fig. S5A and B). Our previous study (13) reported that MYBBP1A inhibited IGFBP5 transcription by promoting the high methylation level of CpG island at IGFBP5 CDS sites. Then, the Methprimer database was used to predict the methylation sites of IGFBP4 and found that there were CpG islands in the promoter region of IGFBP4 (Fig. 5F). The SMART database was used to analyze the correlation between IGFBP4 methylation and expression and it was found that the expression of IGFBP4 was significantly negatively associated with the methylation in transcription level (Fig. 5G). In addition, a higher level of IGFBP4 promoter methylation was observed in patients with higher tumor grade and stage (Fig. 5H and I). Bisulfite sequencing PCR (BSP) technology was utilized to compare the methylation levels of CpG islands in the IGFBP4 promoter region between the MYBBP1A knocked-down group and the NC group (Fig. 5J). Overall methylation in the IGFBP4 promoter region was decreased in the MYBBP1A knockdown group compared with the control group. More importantly, mRNA levels of IGFBP4 in HCC cells were significantly increased after treatment with DNA methyltransferase inhibitor Decitabine (5-Aza-2'-deoxycytidine) (0, 5, 10 and 40 $\mu\text{mol/l}$) (Fig. 5K and L). The inhibitory efficiency of 5Aza was verified by detecting the expression of DNMT1 at different concentrations of 5Aza. These results all confirmed that MYBBP1A affects the expression level of IGFBP4 by promoting CpG island methylation of the IGFBP4 promoter region.

Knocking down IGFBP4 restores the repressed metastasis ability of liver cancer caused by MYBBP1A inhibition. To further confirm our theory, lentivirus-mediated shRNA targeting MYBBP1A was used to construct MYBBP1A-knockdown Huh7 and HCCLM3 cells. Transwell and gap closure assay results demonstrated that knocking down MYBBP1A decreased the migratory activities of liver cancer cells (Fig. 6A and B). Then, the lentivirus-mediated shMYBBP1A and shIGFBP4 were used to co-transfect Huh7 and HCCLM3 cells. The results showed that knocking down MYBBP1A suppressed migration ability while knocking down IGFBP4 restored the migration abilities of liver cancer cells (Fig. 6C and D). Besides, colony formation assays revealed that the proliferation ability of liver cancer cells could also be restored (Fig. S6A and B). Moreover, IGFBP4 knockdown could restore the repressed EMT

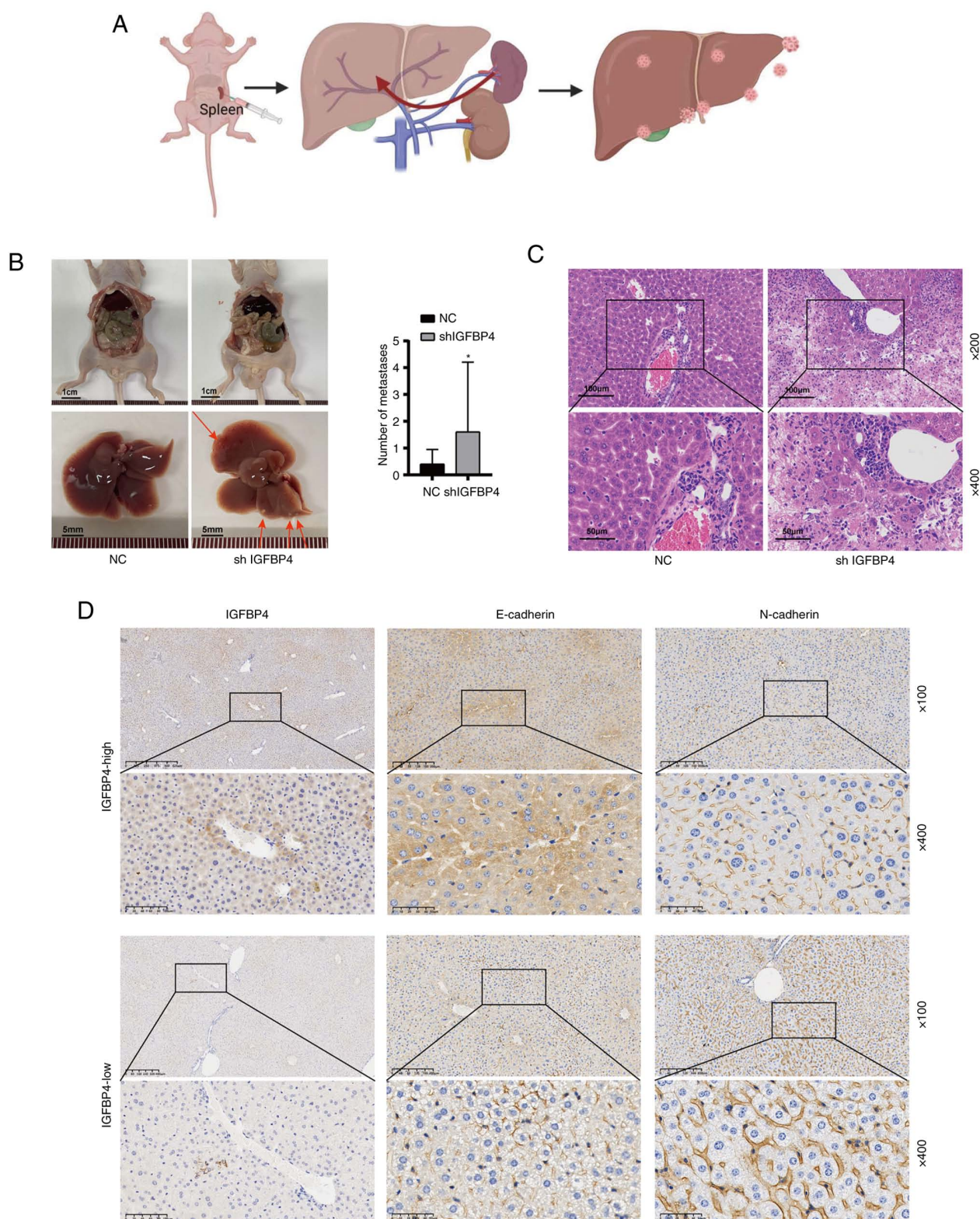


Figure 3. Silencing of IGFBP4 promotes liver cancer metastasis *in vivo*. (A) Illustration of the intra-splenic injection procedure for modeling liver metastasis. (B) More little white liver margins scattered in metastases were observed in the liver of IGFBP4 knockdown group mice compared with the NC group (* $P < 0.05$, Student's t-test). (C) Compared with the NC group, the shIGFBP4 group had more liver cancer metastases, and their representative microscopic morphology was shown by H&E staining (original magnification, x200 and x400). (D) The expression of E-cadherin, N-cadherin and Vimentin in mice liver tissue with IGFBP4-high and IGFBP4-low expression (original magnification, x100 and x400). IGFBP 4, insulin-like growth factor binding protein 4; sh-, short hairpin; NC, negative control.

progression caused by MYBBP1A inhibition. Specifically, inhibition of MYBBP1A increased E-cadherin expression, while knocking down IGFBP4 restricted the increase of

E-cadherin. Similarly, MYBBP1A inhibition decreased N-cadherin expression, and knocking down IGFBP4 restored its expression caused by MYBBP1A inhibition

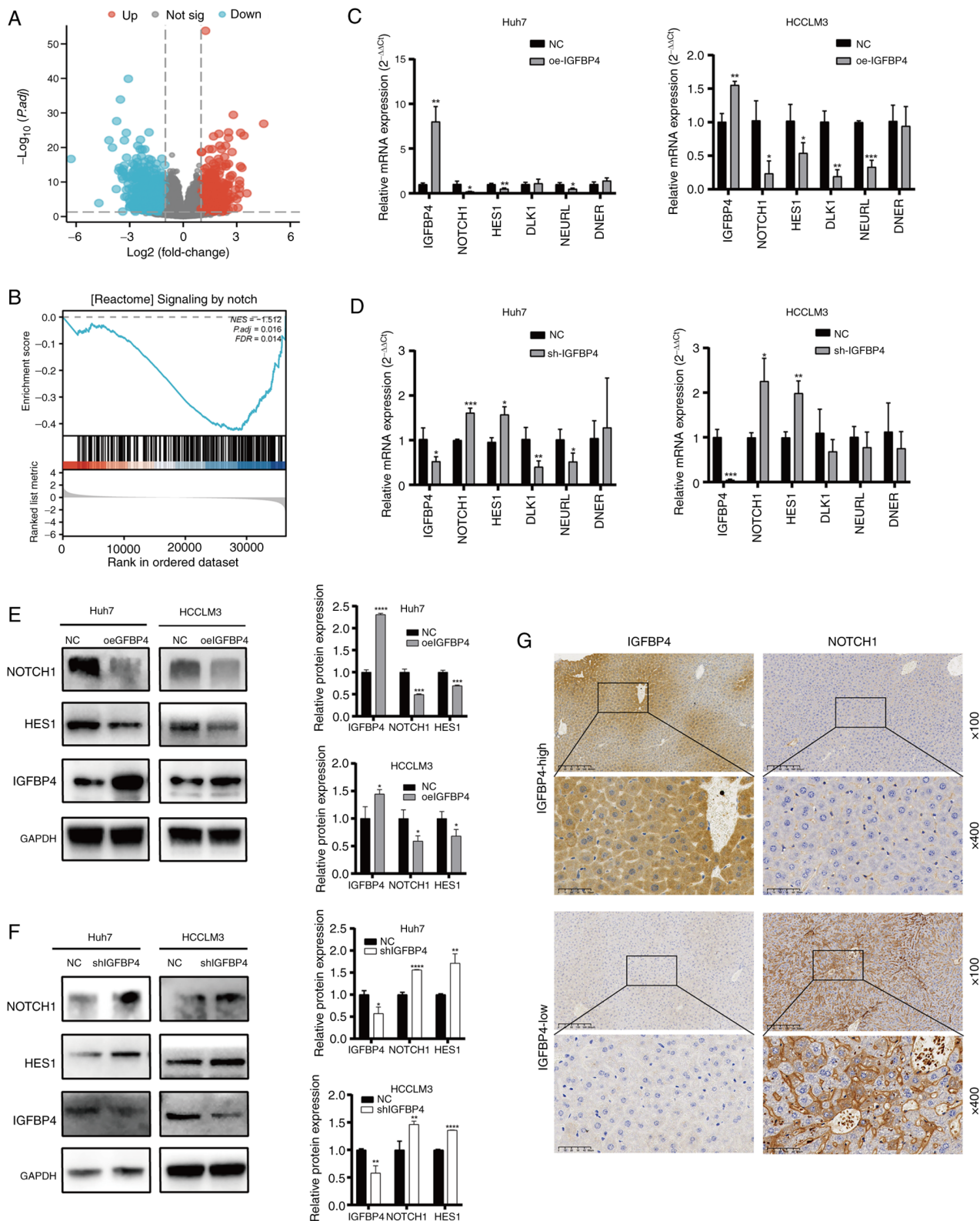


Figure 4. Overexpression of IGFBP4 downregulates NOTCH signaling pathway in liver cancer. (A) Volcano plot of the differentially expressed genes in patients with hepatocellular carcinoma included in The Cancer Genome Atlas database. Red dots represent genes that were significantly upregulated, blue dots represent genes that were significantly downregulated, grey dots represent genes that were not differentially expressed and the horizontal line represents a P-value of 0.05. (B) Gene set enrichment analysis found the differentially expressed gene of IGFBP4 was enriched in the NOTCH signaling pathway (p adj.=0.016, FDR=0.014). (C) The mRNA levels of the NOTCH pathway key genes NOTCH1, HES1 and related genes DLK1, NEURL and DNER in negative control and oeIGFBP4 groups of Huh7 and HCCLM3 cells based on RT-qPCR ($P<0.05$, $^{**}P<0.01$ and $^{***}P<0.001$, Student's t-test). (D) The mRNA levels of NOTCH1, HES1, DLK1, NEURL and DNER in NC and shIGFBP4 groups of Huh7 and HCCLM3 based on RT-qPCR ($P<0.05$, $^{**}P<0.01$ and $^{***}P<0.001$, Student's t-test). (E) The protein expression of NOTCH1 and HES1 in oeIGFBP4 group and NC group in Huh7 and HCCLM3 cell lines based on WB ($P<0.05$, $^{**}P<0.001$, $^{***}P<0.0001$, Student's t-test). (F) The protein expression of NOTCH1 and HES1 in NC and shIGFBP4 group in Huh7 and HCCLM3 cell lines based on WB ($P<0.05$, $^{**}P<0.01$, $^{***}P<0.0001$, Student's t-test). (G) Representative images of immunohistochemical staining of NOTCH1 in the high-expressing IGFBP4 and low-expressing patients with liver tissues (original magnification, x100 and x400). IGFBP4, insulin-like growth factor binding protein 4; HES, hes family bHLH transcription factor 1; NEURL, neuralized E3 ubiquitin protein ligase 1; oe-, overexpression; RT-qPCR, reverse transcription quantitative PCR; NC, negative control; WB, western blotting; sh-, short hairpin.

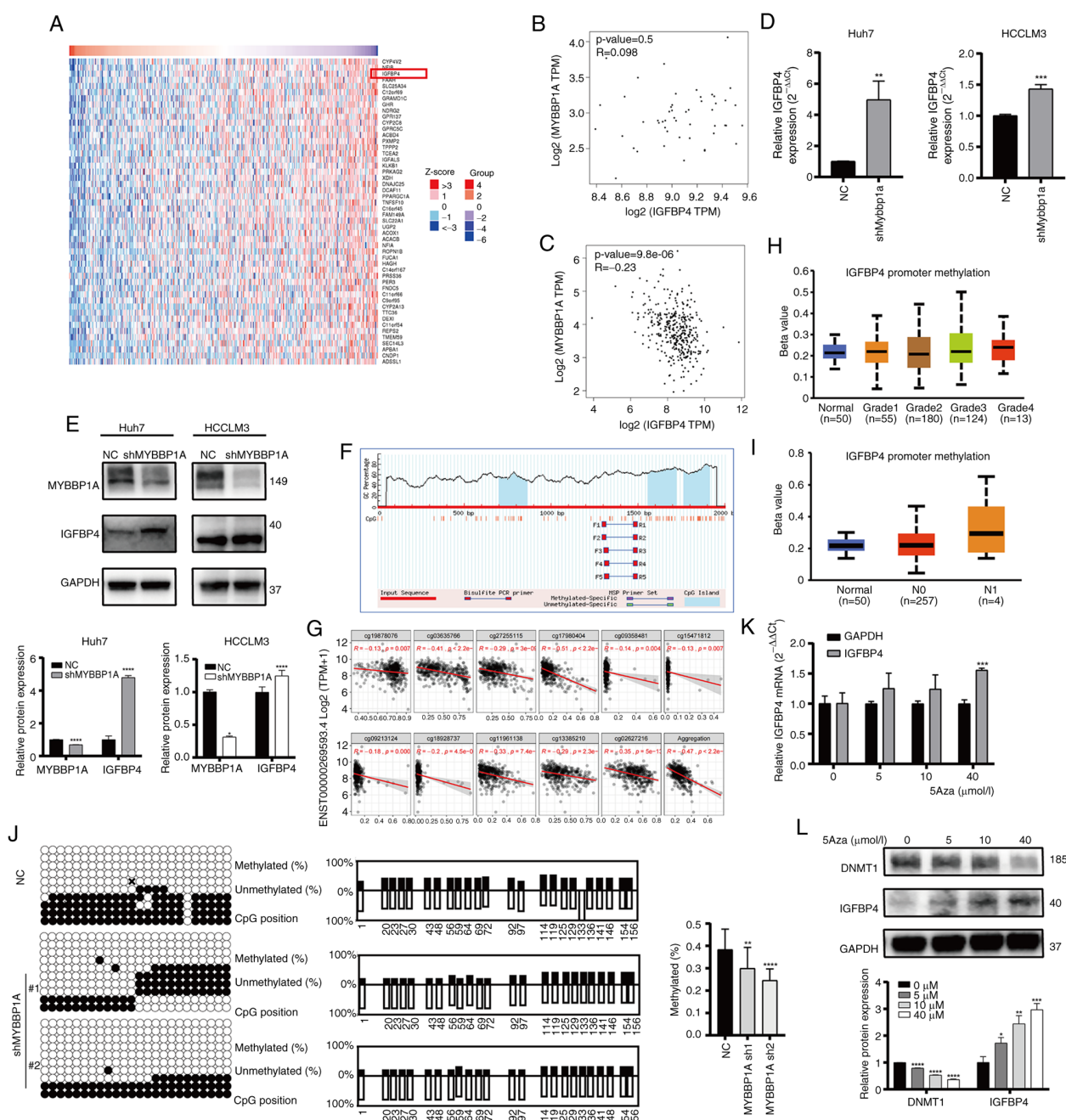


Figure 5. IGFBP4 is negatively regulated by MYBBP1A via CpG island methylation mediated degradation. (A) Heat map showed the top 50 genes which significantly negatively correlated with MYBBP1A from TCGA database, IGFBP4 ranked third. (B and C) TCGA and The Genotype-Tissue Expression databases analysis showed that there was no significant correlation between MYBBP1A and IGFBP4 expression in normal liver tissues ($P=0.05$, $R=0.098$), while there was a negative correlation between MYBBP1A and IGFBP4 expression in patients with liver cancer ($P=9.8\times 10^{-6}$, $R=-0.23$). (D) The expression level of IGFBP4 mRNA in Huh7 and HCCLM3 cell lines after MYBBP1A knockdown was detected by RT-qPCR ($**P<0.01$ and $***P<0.001$, Student's t-test). (E) WB of IGFBP4 protein expression in Huh7 and HCCLM3 cell lines after knockdown of MYBBP1A ($*P<0.05$, $***P<0.0001$, Student's t-test). (F) Using the Methprimer website, three CpG islands were found in the IGFBP4 promoter region. (G) Transcript-level correlation showing that the expression of IGFBP4 is negatively associated with the methylation of cg19878076, cg03635766, cg27255115, cg17980404, cg09358481, cg15471812, cg09213124, cg18928737, cg11961138, cg13385210 and cg02627216 using SMART website analysis (M value, Spearman). (H and I) IGFBP4 promoter methylation level in the liver hepatocellular carcinoma database of TCGA under different tumor grades and lymph node metastases. (J) The methylation level of IGFBP4 promoter region was detected by bisulfite sequencing PCR technique. Compared with the MYBBP1A knockdown group, the IGFBP4 promoter region was more methylated in the control group ($**P<0.01$ and $***P<0.0001$, Student's t-test). (K) The expression level of IGFBP4 mRNA after stimulation with methylase inhibitor 5-Aza at different concentrations (0, 10, 20 and 40 $\mu\text{mol/l}$) after 48 h was detected by RT-qPCR ($***P<0.001$, Student's t-test). (L) WB was performed to detect the expression levels of methylase DNMT1 and IGFBP4 protein after stimulation with different concentrations of methylase inhibitor 5Aza (0, 10, 20, 40 $\mu\text{mol/l}$) after 48 h ($*P<0.05$, $**P<0.01$, $***P<0.001$, $****P<0.0001$, Student's t-test). IGFBP4, insulin-like growth factor binding protein 4; TCGA, The Cancer Genome Atlas; RT-qPCR, reverse transcription-quantitative PCR; WB, western blotting.

(Fig. 6E). As for NOTCH signaling regulation, IGFBP4 knockdown could restore the repressed NOTCH1 and Hes1 expression caused by MYBBP1A inhibition (Fig. 6F).

These results demonstrated that IGFBP4 was involved in regulating EMT, cancer metastasis and EMT and NOTCH activation mediated by MYBBP1A in liver cancer.

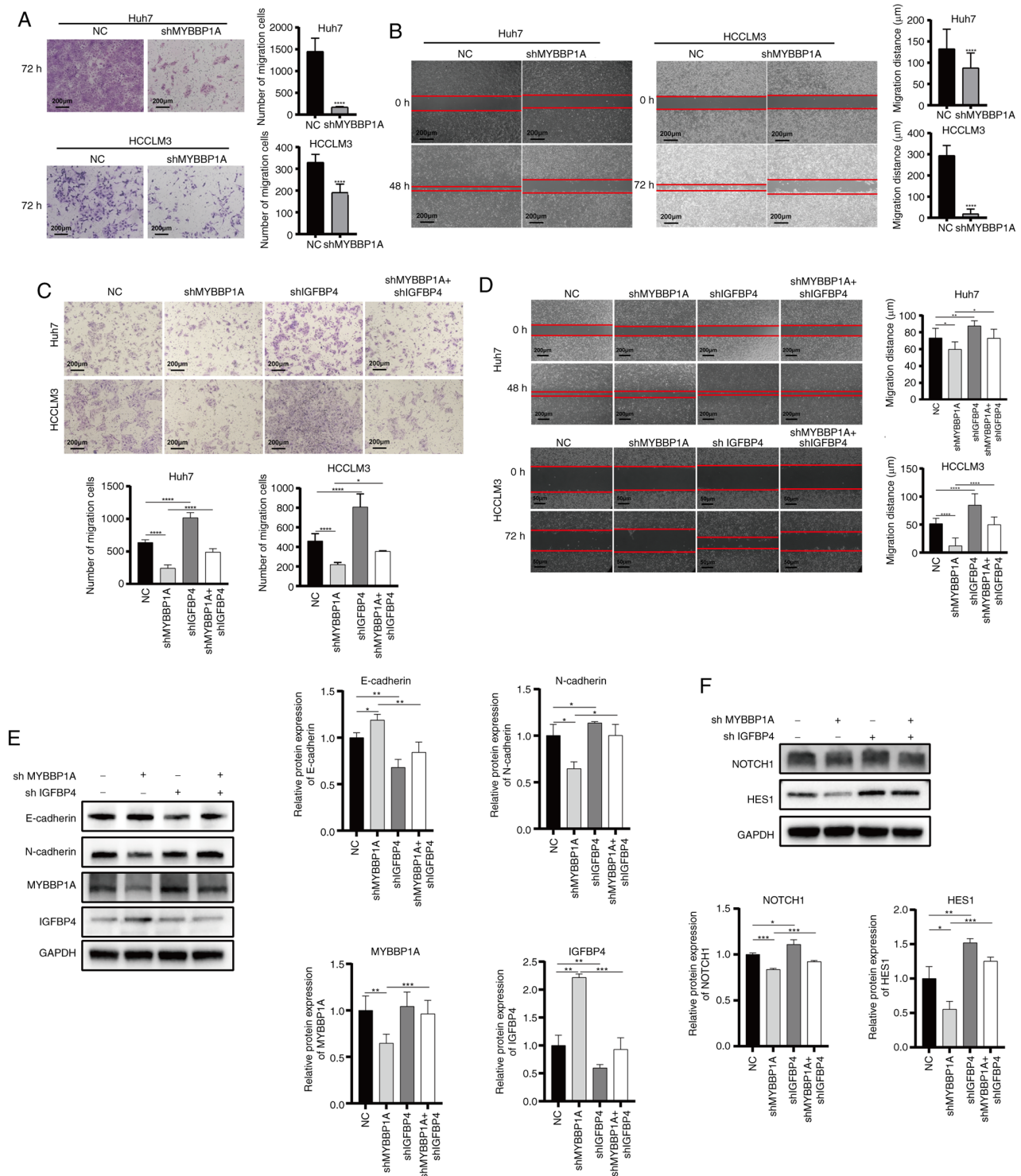


Figure 6. Knocking down IGFBP4 reduces the metastasis ability of liver cancer cell with MYBBP1A low expression. (A and B) The motile activities of shMYBBP1A Huh7 and HCCLM3 cells based on Transwell migration assays and gap closure assays, respectively. (original magnification, x400; ****P<0.0001, Student's t-test). (C and D) The migration capacity of Huh7 and HCCLM3 cell lines in the negative control group, shMYBBP1A group, shIGFBP4 group, and shMYBBP1A + shIGFBP4 group were detected by Transwell migration assay and gap closure experiment (magnification, x100 and x400; *P<0.05, **P<0.01 and ****P<0.0001, Student's t-test). (E) WB analysis of the protein expression levels of MYBBP1A, IGFBP4, and EMT related genes in the negative control group, shMYBBP1A group, shIGFBP4 group and shMYBBP1A + shIGFBP4 group (*P<0.05, **P<0.01, ***P<0.001, Student's t-test). (F) WB analysis was performed to detect the protein expression levels of NOTCH pathway-related genes NOTCH1 and HES1 in the negative control group, shMYBBP1A group, shIGFBP4 group, and shMYBBP1A + shIGFBP4 group (*P<0.05, **P<0.01, ***P<0.001, Student's t-test). IGFBP 4, insulin-like growth factor binding protein 4; sh-, short hairpin; WB, western blotting; NC, negative control; HES, hes family bHLH transcription factor 1.

Clinical significance of IGFBP4 and MYBBP1A in the prognosis of metastatic liver cancer. Overall survival (OS) time and disease-specific survival time (DSS) of patients with liver

cancer with different IGFBP4 expression groups in different tumor grades and stages were analyzed. The results demonstrated that high expression of IGFBP4 was correlated with

longer OS [log-rank $P=3.3 \times 10^{-6}$, hazard ratio (HR)=0.43] and DSS (log-rank $P=2.9 \times 10^{-5}$, HR=0.38). This association was statistically significant in late stages (stages III and IV; log-rank $P=0.0013$ in OS and log-rank $P=0.0012$ in DSS) but not in early stages (stages I and II; log-rank $P=0.047$ in OS and log-rank $P=0.052$ in DSS) in liver cancer (Fig. 7A). Interestingly, the negative correlation between MYBBP1A expression and OS (log-rank $P=0.0045$) or DSS (log-rank $P=0.018$) was observed in late stages (stages III and IV) rather than in early stages (stage I and II) in liver cancer (Fig. 7B). IHC staining was performed on tumor and peritumor tissue specimens of patients with liver cancer with different metastatic status in The First Affiliated Hospital of Zhejiang University. The results suggested that IGFBP4 expression levels in the liver tissues of patients with liver cancer were lower than those in normal individuals, and even lower in patients with metastatic liver cancer (Fig. 7C). Then, the survival curves of patients with HCC with MYBBP1A^{High}IGFBP4^{Low}, MYBBP1A^{High}IGFBP4^{High}, MYBBP1A^{Low}IGFBP4^{High} and MYBBP1A^{Low}IGFBP4^{Low} were analyzed; the results revealed that the OS of patients with MYBBP1A^{High}IGFBP4^{Low} was significantly poorer than those with MYBBP1A^{Low}IGFBP4^{High}. The MYBBP1A^{Low}IGFBP4^{High} group had the most favorable OS in these four groups (Figs. 7D and S8). Therefore, it is concluded that IGFBP4 and MYBBP1A expression could serve as potential biomarkers in predicting the prognosis of liver cancer.

Discussion

The progression of HCC is associated with the abnormal activation of multiple signaling pathways, including angiogenesis, cell proliferation, apoptosis, invasion and metastasis. Current therapies inhibit the proliferation and survival of tumor cells by targeting specific molecules in these abnormal signaling pathways, which rely on specific therapy under molecular targeted diagnosis. While the therapy under the molecular targeted diagnosis has made some progress in the treatment of metastatic liver cancer, there are still challenges (27,28). Novel diagnosis and treatment are getting increasing attention in clinical practice, and the development of treatment strategies based on individualized diagnosis will help improve the treatment effect and provide patients with an improved chance of survival.

IGFBPs are a family of proteins that bind to IGFs and are usually composed of seven high-affinity IGFBP isoforms, namely IGFBP1 to IGFBP7 (7). IGFBP4, the smallest protein in the IGFBP family (29), is a secreted protein mainly produced by the liver (30). It acts as a transport protein for IGF-I and IGF-II and regulates their biological effects. The levels and expression of IGFBP4 in various tissues are influenced by IGFBP proteinases, multiple growth factors and hormones. The results of the present study suggested that IGFBP4 may play a positive regulatory role in the process of tumor cell metastasis and invasion. Overexpression of IGFBP4 in glioblastoma cells leads to the upregulation of molecules involved in tumor growth (31). Inhibition of IGFBP4 could significantly reduce the invasion and expression of mesenchymal markers in oral squamous cell carcinoma (32). Several studies have found that overexpression of IGFBP4 inhibits the invasiveness of

cancer cells, including lung cancer (33), colorectal cancer (34) and breast cancer (9). Previous research has shown that transcriptional activation of IGFBP4 could inhibit the metastasis of liver cancer (35,36). In the present study, the analysis of the TCGA database and clinical samples from patients with HCC showed that IGFBP4 was downregulated in liver cancer. In addition, despite the lack of 5-10 years of survival data which is the limitation in the present study, the five-year survival curve analysis still showed that the high expression of IGFBP4 was associated with favorable prognosis in patients with HCC. EMT was considered one of the key steps in tumor metastasis and invasion. During EMT, tumor cells could lose the adhesive properties of epithelial cells, acquire the motility of mesenchymal cells, and enter other organs through the blood or lymphatic system. In the present study, comprehensive experimental methods such as gap closure experiments and Transwell assays were used to verify that overexpressing IGFBP4 could inhibit the migration ability of HCC *in vitro* and reduce the tumor metastasis *in vivo*. It was confirmed that overexpression of IGFBP4 in HCC cells leads to upregulation of the epithelial marker protein E-cadherin, downregulation of the mesenchymal marker protein N-cadherin and the cytoskeletal protein Vimentin.

DNA methylation is a common epigenetic modification (37). Aberrant regulation of DNA methylation is closely associated with tumorigenesis and progression in liver cancer (38). High methylation status is associated with gene silencing and functional loss. Studies have shown that some tumor suppressor genes undergo hypermethylation, leading to the methylation of their promoter regions and subsequent gene silencing, thereby causing tumor cells to lose normal proliferation and growth control. Our previous research suggested that IGFBP5 was regulated by MYBBP1A, inducing abnormal hypermethylation of the CpG island in the IGFBP5 CDS region, inhibiting IGFBP5 transcription and secretion which promoted HCC progression (27). It was hypothesized that IGFBP4, another important member of the IGFBP family, may also be regulated by MYBBP1A. To validate this hypothesis, it was firstly confirmed that MYBBP1A indeed promotes the migratory and invasive abilities of liver cancer cells. Secondly, it was demonstrated that IGFBP4 expression is negatively regulated by MYBBP1A, and rescue experiments further confirmed this relationship. Additionally, using Methprimer analysis, it was found that there were CpG islands in the IGFBP4 promoter region, and the methylation level of IGFBP4 was negatively correlated with poor prognosis. To further verify that the high methylation status of the IGFBP4 promoter is regulated by MYBBP1A, BSP was used to confirm that knocking down MYBBP1A leads to a decrease in CpG island methylation in the IGFBP4 promoter regions and an enhancement of target gene transcription. Furthermore, treatment with the methylation inhibitor 5-Aza resulted in a subsequent decrease in IGFBP4 expression.

EMT is a dynamic process that can be achieved through multiple signaling pathways such as IGF-1R receptor ligand activation, NOTCH, Wnt/ β -catenin and Hedgehog pathway activation, which may also contribute to the EMT process. Studies have shown that knocking down Wnt3a can affect the activation of the Wnt/ β -catenin signaling pathway,

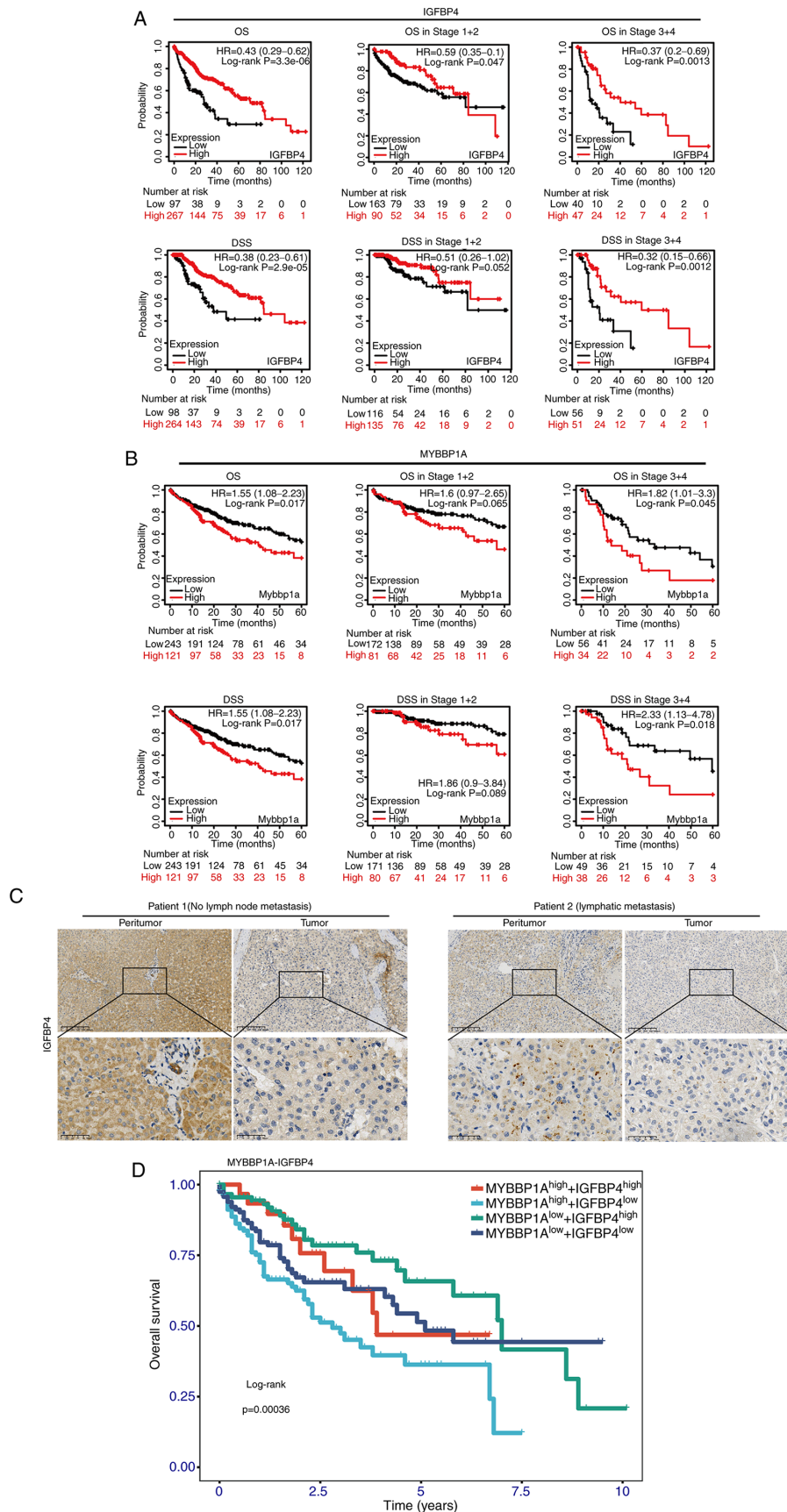


Figure 7. Clinical significance of IGFBP4 and MYBBP1A in prognosis of liver cancer. (A and B) Kaplan Meier-plotter database website analyzed OS and DSS of patients with liver cancer in different IGFBP4 and MYBBP1A expression groups at different tumor grade stages (Log Rank Mantel-Cox). (C) Immunohistochemical staining showed different expression of IGFBP4 in hepatocellular carcinoma tissues and adjacent tissues of patients with/without tumor metastasis. (D) Kaplan Meier survival curve showed the results among the MYBBP1A^{High}IGFBP4^{High}, MYBBP1A^{High}IGFBP4^{Low}, MYBBP1A^{Low}IGFBP4^{High} and MYBBP1A^{Low}IGFBP4^{Low} group [P=0.00036 respectively, Log Rank (Mantel-Cox)]. The cut-off values were determined using the surv_cutpoint function from the survminer package, yielding 438.9 for IGFBP4 and 6.29 for MYBBP1A. IGFBP4, insulin-like growth factor binding protein 4; OS, overall survival; DSS, disease specific survival.

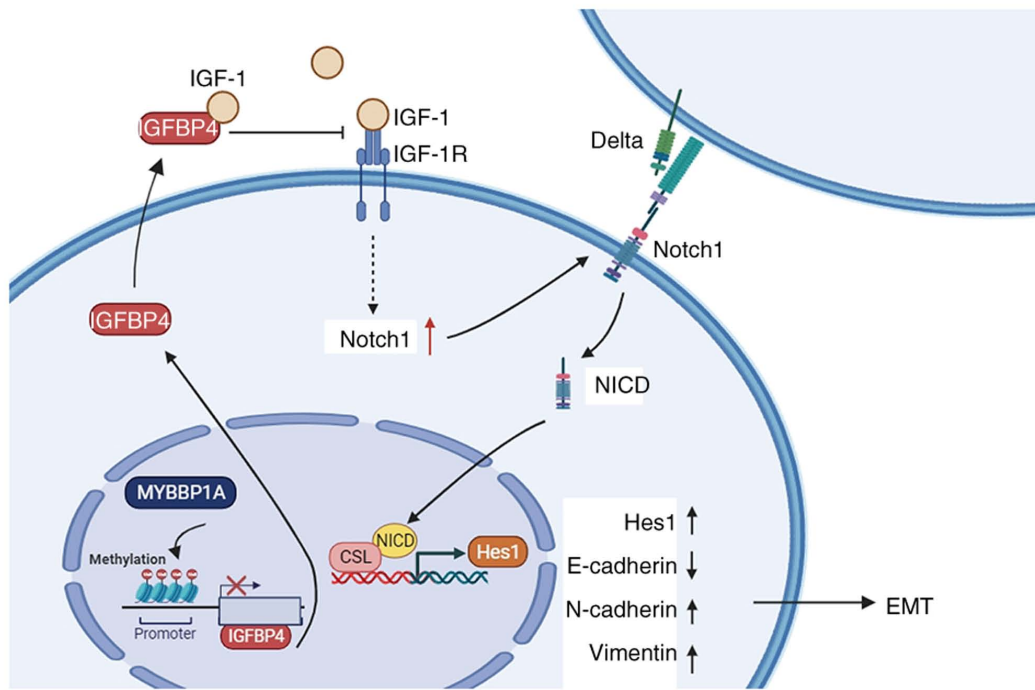


Figure 8. Molecular models describing the mechanism of IGFBP4 as a tumor suppressor gene in liver cancer. IGFBP 4, insulin-like growth factor binding protein 4; EMT, epithelial-mesenchymal transition.

thereby affecting the EMT process and inhibiting the metastatic ability of liver cancer cells (39,40). Initially, it was considered that IGFBP4 function was closely associated with the Wnt/ β -catenin pathway. WB assays were performed to assess the expression of β -catenin/Wnt3a/Smad protein. However, no significant changes in the expression of these proteins were observed following IGFBP4 overexpression (Fig. S3). This result may be attributed to the complex crosstalk between signaling pathways, suggesting that the β -catenin/Smad pathway may not serve as the primary driver in this regulatory axis. Further investigation supports that this pathway is likely not the predominant mechanism by which IGFBP4 influences liver cancer metastasis. Through GSEA analysis, differential gene enrichment was found in the NOTCH pathway, which is another crucial pathway that affects the EMT. The NOTCH signaling pathway was aberrantly activated in various tumors and has been found to be associated with tumor cell proliferation, invasion and metastasis (41). In pancreatic cancer, RHBDL2 stabilizes NICD through OTUD7B and activates the NOTCH signaling pathway, promoting cell proliferation and migration (42). In the liver, activation of the NOTCH-YAP1/TEAD-DNMT1 axis drives hepatocytes to develop into intrahepatic cholangiocarcinoma (43). When the NOTCH1 receptor binds to the DELTA ligand, the extracellular structure of the receptor undergoes conformational changes, leading to the cleavage of the receptor's intracellular domain (NICD) by γ -secretase. NICD is further translocated into the nucleus and forms a transcriptional regulatory complex with the key transcription factor CSL, promoting the transcription of downstream target genes (44). Hes1 is one of the downstream target genes of the NOTCH signaling pathway, and its expression is regulated by the NICD-CSL complex. In

the present study, overexpression of IGFBP4 was found to significantly increase the transcription and protein levels of NOTCH1 and its downstream target gene Hes1. Some studies showed that EMT and IGF-1R activation are involved in a positive feedback loop (45). IGFBP4 can bind to IGF1, inhibit the binding of IGF ligands to the receptor, and prolong its half-life in circulation (46). The crosstalk between IGF-1R and NOTCH could jointly act on the EMT phenotype of tumors. Some researchers considered that IGF-1R was a target of NOTCH1, and NOTCH directly upregulated the expression of IGF1R in human T-cell acute lymphoblastic leukemia cells, significantly enhancing their sensitivity to environmental ligands (47). It has also been suggested that NOTCH1 may be transcriptionally activated by YAP (48,49) and the activity of this transcription factor is triggered by the IGF-1R/PI3K/mTOR signaling pathway. Additionally, the YAP-IGF1R signaling loop is also involved in EMT-related proteins (50,51). The results of protein interaction analysis showed that IGFBP4 had a strong interaction with IGF1/IGF1R, and IGF1R also showed a strong interaction with NOTCH1 and YAP1 (Fig. S7). The present study confirmed that the overexpression of IGFBP4 significantly reduces the level of the transcription factor YAP, which is positively correlated with the activation of the NOTCH pathway (Fig. S4). Regrettably, the specific mechanism by which IGFBP4 regulates the NOTCH pathway through YAP was not investigated. Further studies, along with additional clinical sample data, are required to confirm the upstream and downstream regulatory effects of IGFBP4 on the NOTCH pathway. This topic could serve as a significant focus for future research.

The previous phase of our research (13) elucidated the mechanism of MYBBP1A regulates IGFBP5 transcription

and inhibits the AKT pathway, and it was hypothesized that another member of the family, IGFBP4, may have a similar function. Since IGFBP4 has been found to play an important role in other cancers, experiments were designed to verify the function of IGFBP4 and its upstream and downstream pathways in HCC. In conclusion, IGFBP4 is a potent biomarker that plays a protective role in liver cancer, especially in metastatic liver cancer. By exploring the upstream and downstream of IGFBP4, it was revealed that MYBBP1A inhibits the transcription of IGFBP4 through high methylation levels of the CpG islands of the IGFBP4 promoter region mediated by DNMT1, which promotes the activation of the NOTCH pathway, increasing the EMT of HCC and providing migration ability for cancer cells (Fig. 8). A recent study by the authors showed that liver cancer populations with high MYBBP1A expression had a poor prognosis (27), and subsequently, it was found that low expression of IGFBP4 in HCC was associated with poor prognosis in patients with HCC. Therefore, a combined prognostic analysis of MYBBP1A and IGFBP4 was performed. It was found that MYBBP1A^{High}IGFBP4^{High} patients had an improved prognosis than MYBBP1A^{High}IGFBP4^{Low}, and in the population with high MYBBP1A expression and poor prognosis, high IGFBP4 expression at the same time could prolong the OS time. It was also found that MYBBP1A^{Low}IGFBP4^{Low} patients had an improved prognosis than those with MYBBP1A^{High}IGFBP4^{Low}, and in populations with high MYBBP1A expression and poor prognosis, simultaneous high expression of IGFBP4 could prolong OS. Similarly, among the four groups, MYBBP1A^{Low}IGFBP4^{High} patients had the best prognosis, and the OS of patients with MYBBP1A^{Low}IGFBP4^{High} was significantly longer than those with MYBBP1A^{High}IGFBP4^{Low} (Fig. S8). Dual gene biomarker combination prediction of MYBBP1A and IGFBP4 has great potential in the prognosis of metastatic liver cancer, providing a theoretical basis for the precise treatment and survival prediction of liver cancer.

The primary limitations of the present study are the restricted sample size and the absence of longitudinal prognostic data. Future studies with larger cohorts will be essential to confirm these observations. Further research should also aim to elucidate the specific mechanisms by which IGFBP4 regulates the NOTCH pathway in liver cancer and explore the roles of other IGFBP family members in hepatocarcinogenesis, as they may contribute through distinct or complementary mechanisms.

Acknowledgements

The authors appreciate the kind help from Mr Yonghao Xu, a laboratory technician, from the Experimental Animal Center of the First Affiliated Hospital of Zhejiang University School of Medicine for providing technical support for animal experiments.

Funding

The present study was supported by the National Natural Science Foundation of China (grant nos. 82103487 and 82302893) and the Zhejiang Provincial Natural Science Foundation of China (grant nos. LQ21H160018 and LQ24H160011).

Availability of data and materials

The data generated in the present study may be requested from the corresponding author.

Authors' contributions

YS and XW conceived and designed the study, acquired, analysed and interpreted the data, confirm the authenticity of all the raw data, and participated in drafting or revision of the submitted article. WC, JG, BD, JR and XH acquired, analysed and interpreted the data, and revised the submitted article. DM, YL, SC and RD collected clinical samples, analysed and interpreted data. JR and BY conceived and designed the study, and participated in drafting or revision of the submitted article. All authors read and approved the final version of the manuscript.

Ethics approval and consent to participate

Human studies (approval no. 2020-IIT-834) and animal experiments (approval no. 2020-IIT-rapid-1132) were approved by the Clinical Research Ethics Committee of the First Affiliated Hospital, School of Medicine, Zhejiang University (Hangzhou, China). Written informed consent was obtained by all patients participating in the present study. Animal experiments were performed in strict accordance with the NIH Guide for the Care and Use of Laboratory Animals.

Patient consent for publication

Not applicable.

Competing interests

The authors declare that they have no competing interests.

References

1. Siegel RL, Miller KD, Wagle NS and Jemal A: Cancer statistics, 2023. *CA Cancer J Clin* 73: 17-48, 2023.
2. Sung H, Ferlay J, Siegel RL, Laversanne M, Soerjomataram I, Jemal A and Bray F: Global cancer statistics 2020: GLOBOCAN estimates of incidence and mortality worldwide for 36 cancers in 185 countries. *CA Cancer J Clin* 71: 209-249, 2021.
3. Llovet JM, Kelley RK, Villanueva A, Singal AG, Pikarsky E, Roayaie S, Lencioni R, Koike K, Zucman-Rossi J and Finn RS: Hepatocellular carcinoma. *Nat Rev Dis Primers* 7: 6, 2021.
4. Xia C, Dong X, Li H, Cao M, Sun D, He S, Yang F, Yan X, Zhang S, Li N and Chen W: Cancer statistics in China and United States, 2022: Profiles, trends, and determinants. *Chin Med J (Engl)* 135: 584-590, 2022.
5. Kulik L and El-Serag HB: Epidemiology and management of hepatocellular carcinoma. *Gastroenterology* 156: 477-491.e1, 2019.
6. Yang JD, Hainaut P, Gores GJ, Amadou A, Plymoth A and Roberts LR: A global view of hepatocellular carcinoma: Trends, risk, prevention and management. *Nat Rev Gastroenterol Hepatol* 16: 589-604, 2019.
7. Durai R, Davies M, Yang W, Yang SY, Seifalian A, Goldspink G and Winslet M: Biology of insulin-like growth factor binding protein-4 and its role in cancer (review). *Int J Oncol* 28: 1317-1325, 2006.
8. Yang B, Zhang L, Cao Y, Chen S, Cao J, Wu D, Chen J, Xiong H, Pan Z, Qiu F, *et al*: Overexpression of lncRNA IGFBP4-1 reprograms energy metabolism to promote lung cancer progression. *Mol Cancer* 16: 154, 2017.

9. Chen W, Hu L, Lu X, Wang X, Zhao C, Guo C, Li X, Ding Y, Zhao H, Tong D, *et al*: The RNA binding protein MEX3A promotes tumor progression of breast cancer by post-transcriptional regulation of IGFBP4. *Breast Cancer Res Treat* 201: 353-366, 2023.
10. Li C, Cao Y, Zhang L, Li J, Wu H, Ling F, Zheng J, Wang J, Li B, He J, *et al*: LncRNA IGFBP4-1 promotes tumor development by activating Janus kinase-signal transducer and activator of transcription pathway in bladder urothelial carcinoma: Retraction. *Int J Biol Sci* 19: 4833, 2023.
11. Conover CA: Insulin-like growth factor-binding proteins and bone metabolism. *Am J Physiol Endocrinol Metab* 294: E10-E14, 2008.
12. Maridas DE, DeMambro VE, Le PT, Mohan S and Rosen CJ: IGFBP4 is required for adipogenesis and influences the distribution of adipose depots. *Endocrinology* 158: 3488-3500, 2017.
13. Weng X, Wu J, Lv Z, Peng C, Chen J, Zhang C, He B, Tong R, Hu W, Ding C, *et al*: Targeting MYBBP1A suppresses HCC progression via inhibiting IGF1/AKT pathway by CpG islands hypo-methylation dependent promotion of IGFBP5. *EBioMedicine* 44: 225-236, 2019.
14. Livak KJ and Schmittgen TD: Analysis of relative gene expression data using real-time quantitative PCR and the 2(-Delta Delta C(T)) Method. *Methods* 25: 402-408, 2001.
15. Ru J, Lu J, Ge J, Ding B, Su R, Jiang Y, Sun Y, Ma J, Li Y, Sun J, *et al*: IRGM is a novel regulator of PD-L1 via promoting S6K1-mediated phosphorylation of YBX1 in hepatocellular carcinoma. *Cancer Lett* 581: 216495, 2024.
16. Hu X, Chen G, Huang Y, Cheng Q, Zhuo J, Su R, He C, Wu Y, Liu Z, Yang B, *et al*: Integrated multiomics reveals silencing of has_circ_0006646 Promotes TRIM21-Mediated NCL ubiquitination to inhibit hepatocellular carcinoma metastasis. *Adv Sci (Weinh)* 11: e2306915, 2024.
17. Workman P, Aboagye EO, Balkwill F, Balmain A, Bruder G, Chaplin DJ, Double JA, Everitt J, Farningham DA, Glennie MJ, *et al*: Guidelines for the welfare and use of animals in cancer research. *Br J Cancer* 102: 1555-1577, 2010.
18. Sugase T, Lam BQ, Danielson M, Terai M, Aplin AE, Gutkind JS and Sato T: Development and optimization of orthotopic liver metastasis xenograft mouse models in uveal melanoma. *J Transl Med* 18: 208, 2020.
19. Purohit A, Saxena S, Varney M, Prajapati DR, Kozel JA, Lazenby A and Singh RK: Host Cxcr2-Dependent regulation of pancreatic cancer growth, angiogenesis, and metastasis. *Am J Pathol* 191: 759-771, 2021.
20. Seki K, Yamaguchi A, Goi T, Nakagawara G, Matsukawa S, Urano T and Furukawa K: Inhibition of liver metastasis formation by anti-CD44 variant exon 9 monoclonal antibody. *Int J Oncol* 11: 1257-1261, 1997.
21. Ohta T, Futagami F, Tajima H, Kitagawa H, Kayahara M, Nagakawa T, Miwa K, Yamamoto M, Iseki S, Nakanuma Y and Terada T: Inhibitory effect of a serine protease inhibitor, FOY-305 on the invasion and metastasis of human pancreatic cancers. *Int J Oncol* 11: 813-817, 1997.
22. Takesue S, Ohuchida K, Shinkawa T, Otsubo Y, Matsumoto S, Sagara A, Yonenaga A, Ando Y, Kibe S, Nakayama H, *et al*: Neutrophil extracellular traps promote liver micrometastasis in pancreatic ductal adenocarcinoma via the activation of cancer-associated fibroblasts. *Int J Oncol* 56: 596-605, 2020.
23. Tauriello DVF, Palomo-Ponce S, Stork D, Berenguer-Llargo A, Badia-Ramentol J, Iglesias M, Sevillano M, Ibiza S, Cañellas A, Hernando-Momblona X, *et al*: TGF β drives immune evasion in genetically reconstituted colon cancer metastasis. *Nature* 554: 538-543, 2018.
24. Wang Z, Li Y, Kong D and Sarkar FH: The role of NOTCH signaling pathway in epithelial-mesenchymal transition (EMT) during development and tumor aggressiveness. *Curr Drug Targets* 11: 745-751, 2010.
25. Yang X, Bai Q, Chen W, Liang J, Wang F, Gu W, Liu L, Li Q, Chen Z, Zhou A, *et al*: m(6) A-Dependent Modulation via IGF2BP3/MCM5/NOTCH Axis Promotes Partial EMT and LUAD Metastasis. *Adv Sci (Weinh)* 10: e2206744, 2023.
26. Yuan X, Wu H, Han N, Xu H, Chu Q, Yu S, Chen Y and Wu K: NOTCH signaling and EMT in non-small cell lung cancer: Biological significance and therapeutic application. *J Hematol Oncol* 7: 87, 2014.
27. Finn RS, Qin S, Ikeda M, Galle PR, Ducreux M, Kim TY, Kudo M, Breder V, Merle P, Kaseb AO, *et al*: Atezolizumab plus bevacizumab in unresectable hepatocellular carcinoma. *N Engl J Med* 382: 1894-1905, 2020.
28. Xu L, Shao Z, Fang X, Xin Z, Zhao S, Zhang H, Zhang Y, Zheng W, Yu X, Zhang Z and Sun L: Exploring precision treatments in immune-mediated inflammatory diseases: Harnessing the infinite potential of nucleic acid delivery. *Exploration* 202: 30165, 2024.
29. Sato H, Sakaeda M, Ishii J, Kashiwagi K, Shimoyamada H, Okudela K, Tajiri M, Ohmori T, Ogura T, Woo T, *et al*: Insulin-like growth factor binding protein-4 gene silencing in lung adenocarcinomas. *Pathol Int* 61: 19-27, 2011.
30. Mazerbourg S, Callebaut I, Zapf J, Mohan S, Overgaard M and Monget P: Up date on IGFBP-4: Regulation of IGFBP-4 levels and functions, in vitro and in vivo. *Growth Horm IGF Res* 14: 71-84, 2004.
31. Praveen Kumar VR, Sehgal P, Thota B, Patil S, Santosh V and Kondaiah P: Insulin like growth factor binding protein 4 promotes GBM progression and regulates key factors involved in EMT and invasion. *J Neurooncol* 116: 455-464, 2014.
32. Ma X, Zhao D, Liu S, Zuo J, Wang W, Wang F, Li Y, Ding Z, Wang J and Wang X: FERMT2 upregulation in CAFs enhances EMT of OSCC and M2 macrophage polarization. *Oral Dis* 30: 991-1003, 2024.
33. Diehl D, Hoeflich A, Wolf E and Lahm H: Insulin-like growth factor (IGF)-binding protein-4 inhibits colony formation of colorectal cancer cells by IGF-independent mechanisms. *Cancer Res* 64: 1600-1603, 2004.
34. Li W, Sun D, Lv Z, Wei Y, Zheng L, Zeng T and Zhao J: Insulin-like growth factor binding protein-4 inhibits cell growth, migration and invasion, and downregulates COX-2 expression in A549 lung cancer cells. *Cell Biol Int* 41: 384-391, 2017.
35. Tao L, Wang Y, Shen Z, Cai J, Zheng J, Xia S, Lin Z, Wan Z, Qi H, Jin R, *et al*: Activation of IGFBP4 via unconventional mechanism of miRNA attenuates metastasis of intrahepatic cholangiocarcinoma. *Hepatol Int* 18: 91-107, 2024.
36. Lee YY, Mok MT, Kang W, Yang W, Tang W, Wu F, Xu L, Yan M, Yu Z, Lee SD, *et al*: Loss of tumor suppressor IGFBP4 drives epigenetic reprogramming in hepatic carcinogenesis. *Nucleic Acids Res* 46: 8832-8847, 2018.
37. Zhang N, Lin C, Huang X, Kolbanovskiy A, Hingerty BE, Amin S, Broyde S, Geacintov NE and Patel DJ: Methylation of cytosine at C5 in a CpG sequence context causes a conformational switch of a benzo[a]pyrene diol epoxide-N2-guanine adduct in DNA from a minor groove alignment to intercalation with base displacement. *J Mol Biol* 346: 951-965, 2005.
38. Hernandez-Meza G, von Felden J, Gonzalez-Kozlova EE, Garcia-Lezana T, Peix J, Portela A, Craig AJ, Sayols S, Schwartz M, Losic B, *et al*: DNA methylation profiling of human hepatocarcinogenesis. *Hepatology* 74: 183-199, 2021.
39. Qi L, Sun B, Liu Z, Cheng R, Li Y and Zhao X: Wnt3a expression is associated with epithelial-mesenchymal transition and promotes colon cancer progression. *J Exp Clin Cancer Res* 33: 107, 2014.
40. Zhang L, He S, Guan H, Zhao Y and Zhang D: Circulating RNA ZFR promotes hepatocellular carcinoma cell proliferation and epithelial-mesenchymal transition process through miR-624-3p/WEE1 axis. *Hepatobiliary Pancreat Dis Int* 23: 52-63, 2024.
41. Jackstadt R, van Hooff SR, Leach JD, Cortes-Lavaud X, Lohuis JO, Ridgway RA, Wouters VM, Roper J, Kendall TJ, Roxburgh CS, *et al*: Epithelial NOTCH signaling rewires the tumor microenvironment of colorectal cancer to drive poor-prognosis subtypes and metastasis. *Cancer Cell* 36: 319-336.e7, 2019.
42. Chen S, Cai K, Zheng D, Liu Y, Li L, He Z, Sun C and Yu C: RHBDL2 promotes the proliferation, migration, and invasion of pancreatic cancer by stabilizing the N1ICD via the OTUD7B and activating the NOTCH signaling pathway. *Cell Death Dis* 13: 945, 2022.
43. Hu S, Molina L, Tao J, Liu S, Hassan M, Singh S, Poddar M, Bell A, Sia D, Oertel M, *et al*: NOTCH-YAP1/TEAD-DNMT1 axis drives hepatocyte reprogramming into intrahepatic cholangiocarcinoma. *Gastroenterology* 163: 449-465, 2022.
44. Kawaguchi K and Kaneko S: NOTCH signaling and liver cancer. *Adv Exp Med Biol* 1287: 69-80, 2021.
45. Sivakumar R, Koga H, Selvendiran K, Maeyama M, Ueno T and Sata M: Autocrine loop for IGF-I receptor signaling in SLUG-mediated epithelial-mesenchymal transition. *Int J Oncol* 34: 329-338, 2009.
46. Baxter RC: Signaling pathways of the insulin-like growth factor binding proteins. *Endocr Rev* 44: 753-778, 2023.
47. Medyouf H, Gusscott S, Wang H, Tseng JC, Wai C, Nemirovsky O, Trumpp A, Pflumio F, Carbonei J, Gottardis M, *et al*: High-level IGF1R expression is required for leukemia-initiating cell activity in T-ALL and is supported by NOTCH signaling. *J Exp Med* 208: 1809-1822, 2011.

48. Totaro A, Castellan M, Di Biagio D and Piccolo S: Crosstalk between YAP/TAZ and NOTCH Signaling. Trends Cell Biol 28: 560-573, 2018.
49. Engel-Pizcueta C and Pujades C: Interplay between NOTCH and YAP/TAZ pathways in the regulation of cell fate during embryo development. Front Cell Dev Biol 9: 711531, 2021.
50. Zhu H, Wang DD, Yuan T, Yan FJ, Zeng CM, Dai XY, Chen ZB, Chen Y, Zhou T, Fan GH, *et al*: Multikinase inhibitor CT-707 targets liver cancer by interrupting the hypoxia-activated IGF-1R-YAP axis. Cancer Res 78: 3995-4006, 2018.
51. Ngo MT, Peng SW, Kuo YC, Lin CY, Wu MH, Chuang CH, Kao CX, Jeng HY, Lin GW, Ling TY, *et al*: A yes-associated protein (YAP) and insulin-like growth factor 1 receptor (IGF-1R) signaling loop is involved in sorafenib resistance in hepatocellular carcinoma. Cancers (Basel) 13: 3812, 2021.



Copyright © 2024 Sun et al. This work is licensed under a Creative Commons Attribution-NonCommercial-NoDerivatives 4.0 International (CC BY-NC-ND 4.0) License.